[lit. bp 189.5 °C (739.2 mm) and n^{25}_D 1.5241 for (±)-**1**[34] and $[\alpha]_D$ +14° (benzene) for (*R*)-**1**[5]; UV max (CH_3OH) 273 (ε 1300), 266 (1200), 260 (780), 254 nm (460) (sh); (hexane) 273 (ε 1800), 267 (1400), 260 (1000), 255 nm (710) (sh); CD (CH_3OH) (*c* 0.0149) $[\theta]_{350}$ ±0, $[\theta]_{290}$ ±0, $[\theta]_{274}$ −1100, $[\theta]_{271}$ −370, $[\theta]_{267}$ −1000, $[\theta]_{261}$ −710 (sh), $[\theta]_{243}$ ±0, $[\theta]_{232}$ ±0, $[\theta]_{222}$ −6000, $[\theta]_{219}$ −4400; (hexane) (*c* 0.0126) $[\theta]_{350}$ ±0, $[\theta]_{277}$ ±0, $[\theta]_{272}$ −780, $[\theta]_{267}$ −550, $[\theta]_{265}$ −1000, $[\theta]_{250}$ ±0.

References and Notes

(1) Part 24: H. E. Smith, E. P. Burrows, and F.-M. Chen, *J. Am. Chem. Soc.*, **100**, 3714 (1978).
(2) (a) Vanderbilt University; (b) Tennessee State University.
(3) Supported by National Science Foundation Grant CHE77-04608.
(4) J. A. Schellman, *Acc. Chem. Res.*, **1**, 144 (1968).
(5) S. D. Allen and O. Schnepp, *J. Chem. Phys.*, **59**, 4547 (1973).
(6) J. H. Brewster and J. G. Buta, *J. Am. Chem. Soc.*, **88**, 2233 (1966).
(7) H. Dickerson and F. S. Richardson, *J. Phys. Chem.*, **80**, 2686 (1976).
(8) H. Rupe, *Justus Liebigs Ann. Chem.*, **369**, 311 (1909).
(9) V. Prelog and H. Scherrer, *Helv. Chim. Acta*, **42**, 2227 (1959).
(10) G. Fodor and G. Csepreghy, *J. Chem. Soc.*, 3222 (1961).
(11) M. A. Bush, T. A. Dullforce, and G. A. Sim, *Chem. Commun.*, 1491 (1969).
(12) W. Leithe, *Chem. Ber.*, **64**, 2827 (1931).
(13) O. Cervinka, M. Kral, and P. Malon, *Collect. Czech. Chem. Commun.*, **41**, 2406 (1976).
(14) H. E. Smith and T. C. Willis, *J. Am. Chem. Soc.*, **93**, 2282 (1971).
(15) R. J. Lorentzen, Ph.D. Dissertation, Purdue University, West Lafayette, Ind., 1971.
(16) V. Ghislandi, A. La Manna, and D. Vercesi, *Farmaco, Ed. Sci.*, **31**, 561 (1976).
(17) G. Snatzke, M. Kajtar, and F. Snatzke in "Fundamental Aspects and Recent Developments in Optical Rotatory Dispersion and Circular Dichroism", F. Ciardelli and P. Salvadori, Ed., Heyden, New York, N.Y., 1973, Chapter 3.4.
(18) E. L. Eliel, P. H. Wilken, and F. T. Fang, *J. Org. Chem.*, **22**, 231 (1957).
(19) A.-M. Weidler and G. Bergson, *Acta Chem. Scand.*, **18**, 1483 (1964).
(20) E. L. Martin, *Org. React.*, **1**, 155 (1942).
(21) J. Grimshaw and P. G. Millar, *J. Chem. Soc. C*, 2324 (1970).
(22) J. Almy and D. J. Cram, *J. Am. Chem. Soc.*, **91**, 4459 (1969).
(23) F. B. Clough, Ph.D. Dissertation, Princeton University, Princeton, N.J., 1950.
(24) The configurational designator for the enantiomer of **10** used in ref 15 should be *R* rather than *S*.
(25) W. H. Inskeep, D. W. Miles, and H. Eyring, *J. Am. Chem. Soc.*, **92**, 3866 (1970).
(26) J. Del Bene and H. H. Jaffe, *J. Chem. Phys.*, **48**, 1807 (1968).
(27) J. Del Bene, H. H. Jaffe, R. L. Ellis, and G. Kuehnlenz, "CNDO/S-CI Molecular Orbital Calculations with the Complete Neglect of Differential Overlap and Configuration Interaction", Program 174, Quantum Chemistry Program Exchange (QCPE), Indiana University, Bloomington, Ind.
(28) J. Linderberg and J. Michl, *J. Am. Chem. Soc.*, **92**, 2619 (1970).
(29) D. J. Caldwell, Ph.D. Dissertation, Princeton University, Princeton, N.J., 1962; D. J. Caldwell and H. Eyring, *Annu. Rev. Phys. Chem.*, **15**, 281 (1964).
(30) P. A. Snyder, P. M. Vipond, and W. C. Johnson, Jr., *Biopolymers*, **12**, 975 (1973).
(31) L. Bardet, G. Fleury, R. Granger, and C. Sablayrolles, *J. Mol. Struct.*, **2**, 397 (1968).
(32) E. Tannenbaum, E. M. Coffin, and A. J. Harrison, *J. Chem. Phys.*, **21**, 311 (1953).
(33) G. Gottarelli and B. Samori, *J. Chem. Soc. B*, 2418 (1971).
(34) J. Entel, C. H. Ruof, and H. C. Howard, *Anal. Chem.*, **25**, 1303 (1953).

The Properties of Clusters in the Gas Phase. 2. Ammonia about Metal Ions

A. W. Castleman, Jr.,* Paul M. Holland, D. M. Lindsay, and Karen I. Peterson

Contribution from the Department of Chemistry and Chemical Physics Laboratory, CIRES,† University of Colorado, Boulder, Colorado 80309.

Received February 17, 1978

Abstract: Thermochemical properties of cluster ions, involving Li^+ and Na^+ solvated by ammonia, were measured using high-pressure mass spectrometry. Investigation of the equilibria over a wide range of temperature for the reactions $M^+(NH_3)_n + NH_3 \rightleftarrows M^+(NH_3)_{n+1}$ enabled a determination of both the enthalpies and entropies of clustering. With $M = Li^+$, the enthalpies are found to be 33.1, 21.0, 16.5, 11.1, and 9.3 kcal/mol for n = 1, 2, 3, 4, and 5, respectively. For $M = Na^+$, the enthalpies, with n ranging from 0 to 5, are 29.1, 22.9, 17.1, 14.7, 10.7, and 9.7 kcal/mol, respectively. In contrast to our recent results for K^+ and Rb^+, data for both Li^+ and Na^+ show a significant decrease in bond energy for the attachment of the fifth ammonia molecule to a cluster containing four ligands. These findings suggest the existence of a solvation shell of four ligands in the case of both Li^+ and Na^+. Comparison of the bond energies of the monoligand clusters shows that the ammonia molecule bonds more strongly than H_2O for all alkali metal ions. This is consistent with a simple molecular orbital model which is based on the difference in ionization potentials of the metal and ligand. Quantitative account of the relative trends for the difference in the binding of NH_3 and H_2O to Li^+, Na^+, K^+, and Rb^+ is obtained from calculations made with the extended Hückel method.

Introduction

Investigation of the formation, properties, and structure of small clusters in the gas phase represents a very active area of current research. Results of studies, both involving molecules clustered about ions as well as neutral molecules clustered among themselves, are of interest for several reasons. In particular, there is a growing realization that studies of clusters in the gas phase provide requisite data for elucidating the nature and extent of ion–solvent and solute–solvent interactions which are important in solution chemistry.[1,2] The results give detailed information on forces operating in individual complexes, but without interferences arising from the presence of the bulk solvent.

Data on the formation and stability of clusters are also needed in advancing the theory of phase transitions and the attendant phenomenon of nucleation.[3] In addition, the results of such studies are expected to contribute to an understanding of the development of surfaces[4] and the nature of forces involved in the formation of disperse systems[5] such as micelles, colloids, and aerosols.

Research is currently underway in our laboratory on both neutral and ion cluster reactions. The development of high-pressure mass spectrometric methods, which are applicable for measuring the thermodynamic properties of individual ion clusters, has prompted us to devote considerable attention to studies of the interactions of ions with molecules. Since the interaction potentials between ions and polar molecules are well known, ion clusters are particularly amenable to theoretical calculation and the experimental data find immediate value for comparison with theory.

In order to establish the role of chemical bonding in stabi-

† The Cooperative Institute for Research in Environmental Sciences is jointly sponsored by the University of Colorado and NOAA.

0002-7863/78/1500-6039$01.00/0

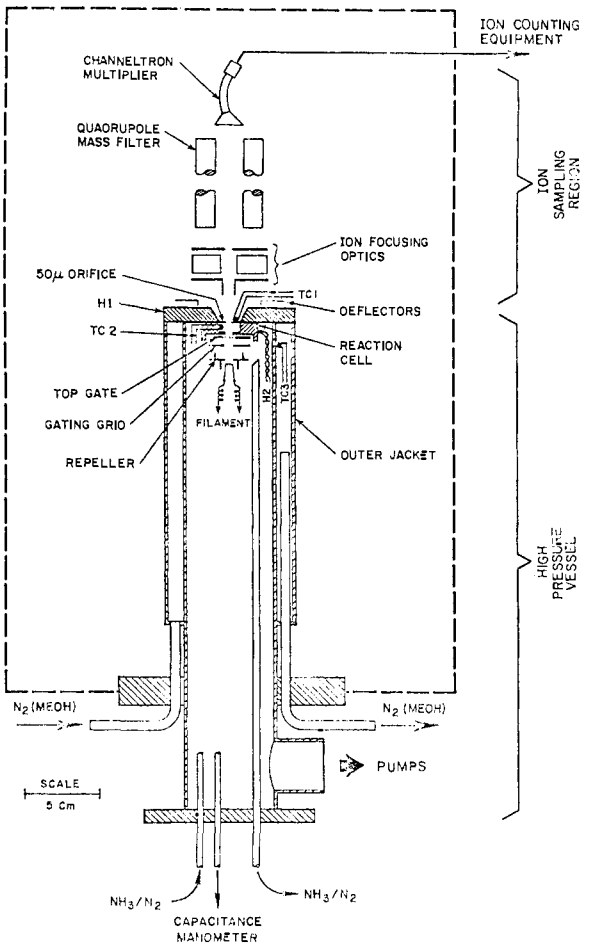

Figure 1. Schematic of the ion clustering apparatus. The figure is drawn approximately to scale, with internal supports omitted for clarity. The broken line in this figure delineates a region of high vacuum. For further discussion refer to the text.

lizing small ion clusters, we have undertaken a systematic study of a number of systems involving ions of both closed and open electronic configuration.[6-10] The results of these studies showed the existence of surprisingly strong bonding for ligand attachment to certain ions, and have suggested the need for further work to elucidate the nature of ligand bonding to a broader class of ions in the gas phase. Earlier data[11] on water molecules clustered to alkali metal ions have been taken[12] as evidence that, in the case of ions having closed electronic configurations, ligand bonding is primarily electrostatic in character. This suggestion is borne out by the ab initio calculations of Clementi and co-workers[13] regarding the attachment of the first cluster of water to both alkali metal and halide ions, and calculations of Woodin et al.[14] for the clustering of both water and ammonia to Li^+.

In contrast, studies made with ions of open electronic configuration have indicated that bonding of ligands to these ions may be partially covalent in character.[6,7,9,10] These results clearly reveal the need for more data to understand the role of chemical bonding in effecting the stability of ion clusters, especially to elucidate the importance of the properties of the ligand such as size and dipole moment. Studies with ammonia are particularly important in this regard. The NH_3 and H_2O molecules are isoelectronic and their molecular sizes are similar, but ammonia has a lower dipole moment than water, i.e., 1.47[15] compared to 1.87 D,[16] and their polarizabilities are significantly different.

The purpose of this paper is to report data for clusters of ammonia about Na^+ and Li^+, and to compare calculated and experimental results for the differences between ammonia and water bond energies to ions of the alkali metal series.

Experimental Section

The ion clustering apparatus is similar to that used in making previous measurements;[6,7,9] important modifications were made to ensure more accurate temperature control and uniform temperatures throughout the reaction cell. Changes were also made in the electronic counting circuit to enable a determination of ion intensities at high count rates.

As shown in Figure 1, positive ions are emitted from a thermionic emission source[17] by application of a positive voltage. The ions are focused by means of a repeller assembly whose potential is set a few volts below that of the filament. Ion energies are further controlled by means of two electrodes, placed before and just inside the reaction cell. The potential of the "top gate" is adjusted to ensure field-free conditions in the reaction cell, where clustering reactions and the final equilibration processes take place.

The high-pressure vessel is constantly recharged with a mixture of NH_3 (Air Products electronic grade, >99.999%) flowing with a buffer gas (in most cases N_2, Air Products U.H.P., >99.998%). Suitable mixtures are prepared several hours in advance of an experimental run and stored in a ballast tank. Mixing ratios employed in these studies ranged from approximately 1 Torr of NH_3, in several hundred torr of N_2 to pure ammonia. Pressure measurements in both the ballast tank and the reaction cell are made with capacitance manometers (MKS Instruments, type 170 M), which are periodically recalibrated in our laboratory.

The temperature of the high thermal conductivity (copper block) reaction cell is established by a combination of electrical heating (H1 and H2 in Figure 1), and controlling the temperature of the jacket surrounding the high-pressure vessel. Chromel-Alumel thermocouples, TC1 and TC2, are used to measure respectively the temperature at the 50-μ orifice and the temperature of the gas just inside the reaction cell. In all measurements, particular attention is given to achieving a uniform temperature distribution throughout the reaction region, and H1 and H2 are adjusted to give TC1 = TC2 ± 0.5 °C. For low-temperature measurements, a large capacity cryostat (Ultra-kryostat, Model UK-75DW) is used to pump cold methanol through the walls of the outer jacket. During operation, the outer jacket temperature, monitored by a third thermocouple, TC3, is held to within 10–15 °C of that in the reaction cell.

The high-pressure vessel is mounted inside a vacuum chamber, delineated by the broken line in Figure 1. A 10-in. diffusion pump plus liquid nitrogen cold trap is used to maintain pressures $< 1 \times 10^{-6}$ Torr in this chamber. As the ions and ion clusters emerge from the high-pressure region, they pass through a four-pole split ring assembly located just after the orifice. This assembly, shown schematically in Figure 1, functions as a deflector and serves to direct the emerging cluster beam into the ion focusing optics. The potential on the first electrode of the ion optics is not allowed to exceed ca. 5 V. The distribution of cluster ions is mass analyzed by a quadrupole mass spectrometer (Extranuclear Laboratories, Model 162-8) and detected by a Channeltron electron multiplier (Galileo Electro-Optics, CEM 4700). The signal from the Channeltron is fed via a new 1-MHz amplifier/discriminator to a multichannel analyzer (Nuclear Data, ND 2400). A mass programmer unit (Extra-nuclear Laboratories, Model 091-3) divides the cluster spectrum into "windows", which are repetitively scanned in synchronization with the multichannel analyzer. Scan times of the order of 1 ms are used in order to minimize the effects of long-term instabilities in the ion source. After a sufficient time to obtain good statistics, the stored counts in each window are integrated to obtain the intensity of each cluster species.

Results

Parameters Influencing the Study of Reaction Equilibria. The applicability of high-pressure mass spectrometry for measuring the thermodynamic properties of cluster ions is now well established.[9,11,18] Nevertheless, certain conditions can lead to a departure from equilibrium. Therefore, it is imperative that the parameters which can influence the attainment of equilibrium, and accurate measurement of the resulting dis-

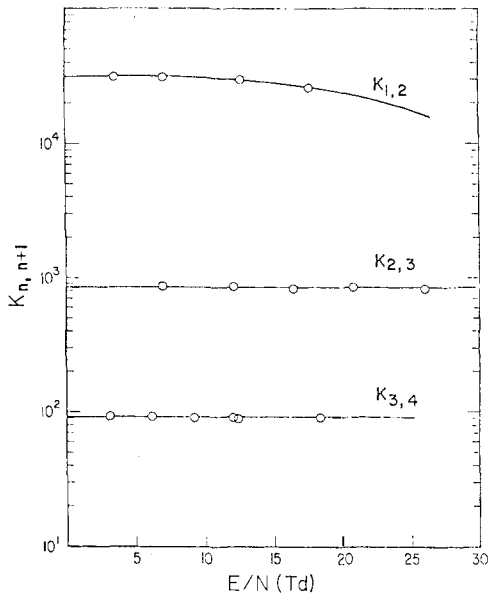

Figure 2. Variation of equilibrium constants, $K_{n,n+1}$, with top gate potential expressed in terms of E/N (ref 20). Units of E/N are townsend; 1 Td = 10^{-17} V cm^{-2}. Temperatures were 349, 261, and 108 °C for $K_{1,2}$, $K_{2,3}$, and $K_{3,4}$, respectively.

tributions, be investigated for each reaction cell geometry and sampling arrangement.

Consider the reaction

$$M^+(B)_n + B \rightleftarrows M^+(B)_{n+1} \quad (1)$$

where $M^+(B)_n$ designates a cluster ion composed of a cation M^+ containing n ligands of constituent B. Equilibrium constants, K, can be expressed in terms of activities, a, of the reactants and products as follows:

$$K_{n,n+1} = a_{n+1}/a_n a_B \cong \frac{I_{n+1}}{I_n}[(p/p^*)_B]^{-1} \quad (2)$$

For the very low concentrations of ions present in the reaction cell, space-charge repulsion is negligible and the ratio of the activities of the ion clusters may be taken as proportional to the ratio of the intensities, I, measured with the mass spectrometer.[19] Likewise, at the very low partial pressures of ligand (millitorr to torr range) as well as total pressures (several torr) employed in the experiments, the systems approach ideal gas behavior. Therefore, the activity of the ligand is equal to its partial pressure p, ratioed to the standard state p^*; here the standard state is taken as 1 atm.

The free energies $\Delta G^\circ_{n,n+1}$, the enthalpies $\Delta H^\circ_{n,n+1}$, and the entropies $\Delta S^\circ_{n,n+1}$ of clustering can be evaluated by measuring the equilibrium constants as a function of temperature for each $[n, n+1]$ reaction according to the following relationships:

$$\Delta G^\circ_{n,n+1} = -RT \ln K_{n,n+1} \quad (3)$$

$$\ln K_{n,n+1} = -(\Delta H^\circ_{n,n+1}/R)T^{-1} + (\Delta S^\circ_{n,n+1}/R) \quad (4)$$

where R is the gas-law constant, and T absolute temperature.

The constant K depends only on temperature and, under conditions where equilibrium is attained, measured ion intensity ratios should be independent of all other variables except the *partial* pressure of the clustering ligand.

In order to ensure that thermodynamic equilibrium is indeed established, and that the measured intensities of the ionic species truly reflect relative concentrations existing in the reaction cell, a number of exploratory experiments were performed.

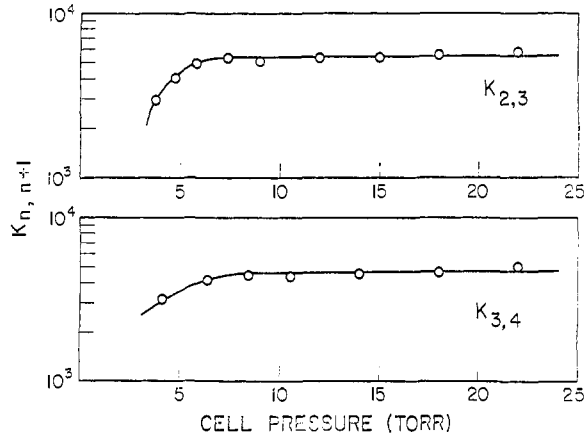

Figure 3. Variation of equilibrium constants, $K_{n,n+1}$, with reaction cell pressure. For $K_{2,3}$ measurements were made at 516 K with a top gate potential of +50 V. The corresponding quantities for $K_{3,4}$ were +60 V and 350 K.

One of the factors which can influence the attainment of equilibrium is ion thermalization. Following emission from the filament, an ion acquires energy from the external electric fields imposed by the various electrodes, and loses energy by collision with gas molecules. The energy that an ion acquires in the external field can be expressed[20] in terms of the ratio of the electric field intensity, E, to the gas number density, N. The values are commonly expressed in units of townsend (Td), where 1 Td = 10^{-17} V cm^{-2}.

In earlier studies[7] we showed that only the first or second cluster reaction is influenced by moderate values of field energy. Essentially the same behavior is found in the recent experiments involving the lithium ion clustered with ammonia. Referring to Figure 2, the measured equilibrium constants $K_{2,3}$ and $K_{3,4}$ can be seen to remain unperturbed for values of $E/N \lesssim 25$ Td. For smaller clusters, departures from true equilibrium conditions become apparent at significantly lower E/N. For example, Figure 2 shows a decreasing value of $K_{1,2}$ for $E/N \gtrsim 10$ Td.

In the case of the addition of the first ammonia ligand to Li^+, one further effect may be noted. Very low ammonia concentrations are required in order to obtain measurable intensities of both Li^+ and Li^+NH_3. In this case, the number of Li^+ collisions with NH_3 is insufficient to establish equilibrium for the reaction:[21]

$$Li^+ + NH_3 + N_2 \rightleftarrows Li^+NH_3 + N_2 \quad (5)$$

This situation is readily discernible from that discussed earlier and evident at large E/N in Figure 2. Departure from equilibrium due to effects related to eq 5 leads to an apparent K which displays an initially steep decrease with E/N. As a consequence of this effect, no reliable measurements of $K_{0,1}$ were obtained for Li^+.

Another factor which requires consideration is the possible dependence of the apparent equilibrium constant on total pressure. Such a dependence would be indicative of (1) failure to achieve ion thermalization, (2) the existence of insufficient collisions for the attainment of clustering equilibrium, or (3) problems with ion sampling. The first two possibilities were discussed in the preceding paragraphs. Evidence that neither cluster breakup nor further clustering occurs with the present ion sampling arrangement has been given in earlier publications.[6-9] Further confirmation is given by the results of Figure 3, where the equilibrium constants $K_{n,n+1}$ are shown to be independent of reaction cell pressure in the range 7-20 Torr. Pressures less than 7 Torr correspond to $E/N \gtrsim 35$ Td where, as discussed previously, equilibrium conditions no longer obtain.

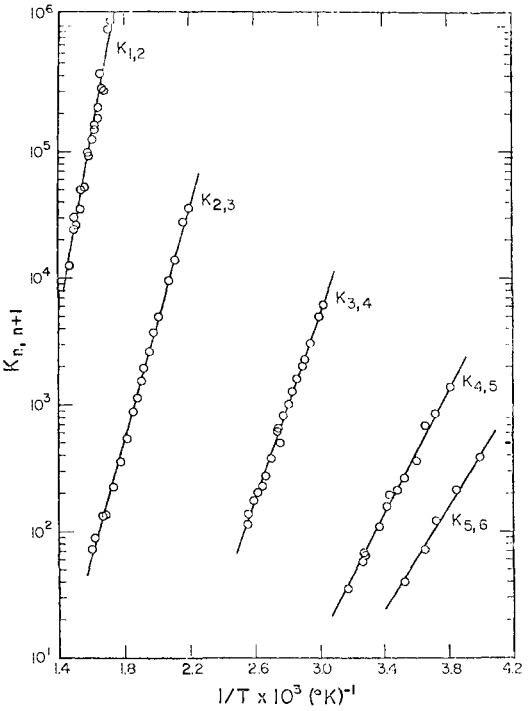

Figure 4. van't Hoff plot, natural logarithm of the equilibrium constant vs. reciprocal absolute temperature, for $Li^+(NH_3)_n + NH_3 \rightleftarrows Li^+(NH_3)_{n+1}$.

Table I. Comparison of Thermodynamic Values for the Reaction $Na^+(H_2O)_3 + H_2O \rightleftarrows Na^+(H_2O)_4$

ref	$-\Delta H°$, kcal/mol	$-\Delta S°$, eu
this work	12.6 ± 0.2[a]	22.0 ± 0.5[a]
9	12.6	23.7
6	13.6	26.0
22	13.8	25.0

[a] Estimated errors correspond to one standard deviation uncertainty in the slope and intercept of the van't Hoff plot of measured equilibrium constants.

Based on the above studies, it is evident that the apparatus, with recent modifications, provides well-defined equilibrium conditions over a wide range of operating parameters. One additional set of experiments was made as final proof that, under appropriate conditions, equilibrium is attained and measured ion populations reflect those present in the reaction cell. Values of $\Delta H°$ and $\Delta S°$ were remeasured for the reaction

$$Na^+(H_2O)_3 + H_2O \rightleftarrows Na^+(H_2O)_4 \quad (6)$$

This reaction was chosen because it has been well characterized by several investigators.[6,9,22] In particular the results provide a basis for comparison with measurements made using the earlier version of the facility previously installed at the Brookhaven National Laboratory. Table I summarizes these data. As can be seen, agreement between the recent work and measurements made at the Brookhaven National Laboratory (ref 9) is excellent. In view of the improved temperature control in the present design, the results reported in ref 6 and 22 (especially the entropy data) are felt to be less accurate than those reported here.

Equilibrium Data for NH_3 Clustered about Li^+ and Na^+. Clustering reactions are expressed by eq 1, where M^+ represents the alkali metal cation (Li^+ or Na^+), and B ammonia. Equilibrium constants, based on eq 2, are presented in the form of van't Hoff plots in Figures 4 and 5 for the respective systems

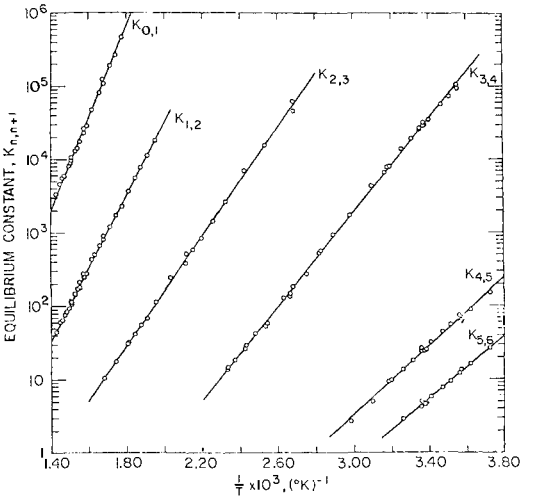

Figure 5. van't Hoff plot, natural logarithm of the equilibrium constant vs. reciprocal absolute temperature, for $Na^+(NH_3)_n + NH_3 \rightleftarrows Na^+(NH_3)_{n+1}$.

Table II. Measured Enthalpies, $\Delta H°_{n,n+1}$, for the Equilibria $M^+(NH_3)_n + NH_3 \rightleftarrows M^+(NH_3)_{n+1}$[b]

	$-\Delta H°_{n,n+1}$, kcal/mol					
M^+	(0,1)	(1,2)	(2,3)	(3,4)	(4,5)	(5,6)
Li^+	38.8[a]	33.1 ±1.3	21.0 ±0.3	16.5 ±0.3	11.1 ±0.3	9.3 ±0.6
Na^+	29.1 ±0.4	22.9 ±0.2	17.1 ±0.2	14.7 ±0.1	10.7 ±0.2	9.7 ±0.2

[a] From R. H. Staley and J. L. Beauchamp, ref 23. Alternate values are 38.4,[14] 39.1,[24] and 38.2 kcal/mol.[25] [b] Estimated errors correspond to one standard deviation uncertainty in the slope of the van't Hoff plots.

Table III. Measured Entropies, $\Delta S°_{n,n+1}$, for the Equilibria $M^+(NH_3)_n + NH_3 \rightleftarrows M^+(NH_3)_{n+1}$[b]

	$-\Delta S°_{n,n+1}$, eu					
M^+	(0,1)	(1,2)	(2,3)	(3,4)	(4,5)	(5,6)
Li^+	23.5[a]	29.7 ±2.1	25.3 ±0.5	32.6 ±0.7	28.0 ±1.0	25.3 ±2.1
Na^+	25.7 ±0.6	25.1 ±0.3	24.0 ±0.3	29.0 ±0.2	29.8 ±0.8	29.7 ±0.7

[a] From ref 24. [b] Estimated errors correspond to one standard deviation uncertainty in the intercept of the van't Hoff plots.

Li^+-NH_3 and Na^+-NH_3. The constants, which span a wide range of values, are well represented by straight lines on these plots.

Employing eq 4 in conjunction with a least-squares analysis computer program, these data were used to deduce the enthalpy and entropy for each of the successive clustering reactions. Enthalpy values are given in Table II for the reactions $(n, n+1)$ with n ranging from zero to five for both the lithium and sodium ions. All but the value of $\Delta H°_{0,1}$ for Li^+ are based on the present results. In the case of the first lithium-ammonia cluster, the tabulated value is based[23] on measurements of the relative stability of ammonia and water clusters of Li^+, and extrapolation of measured values for Li^+ clustered with H_2O. The value is in good agreement with another based on a similar measurement[24] and others[14,25] deduced from theoretical calculations. Entropy data for NH_3 clustered with Li^+ and Na^+ are given in Table III. The magnitudes of the values are similar[10] to those for NH_3 clustered about other alkali metals K^+ and Rb^+.

Considerations of Cluster Bonding and Structure. The enthalpy and entropy data find direct application in under-

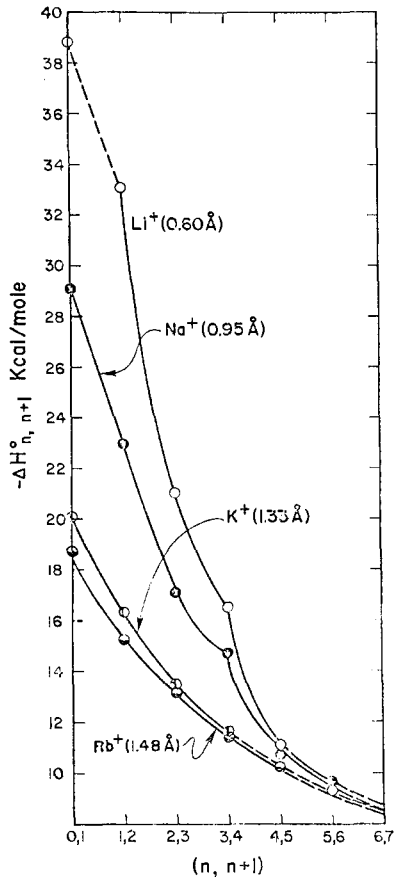

Figure 6. Plot of $\Delta H^\circ_{n,n+1}$ vs. cluster size for the reaction $M^+(NH_3)_n + NH_3 \rightleftarrows M^+(NH_3)_{n+1}$.

standing the bonding and structure of ion clusters. In Figure 6, a plot of enthalpy (directly related to bond energy) vs. cluster size is given for the results of the present work and those of the other alkali metals reported[10] earlier. Displayed in this manner, the data reveal several interesting features. In the case of all alkali metal ions, $\Delta H^\circ_{n,n+1}$ is seen to decrease monotonically with cluster size; furthermore, the enthalpy for any particular cluster reaction can be seen to vary inversely with ionic radius. However, in direct contrast to the situation for the larger alkali-metal ions, where there is a smooth variation with the cluster size, both the Na^+ and Li^+ systems show the presence of a significant decrease in bond energy between the fourth and fifth NH_3 cluster. This effect has not been observed[22] in the case of water clustered about alkali-metal ions, but has been reported[26] for H_2O about NH_4^+ and is evident[9] in going from the eighth to the ninth cluster in the hydration of the Sr^+ ion.

These data suggest that a well-defined "coordination shell" may exist for some ion-ligand systems in the gas phase. Interestingly, the results of Raman spectra studies with Li^+ in liquid ammonia[27] also indicate that the coordination number of Li^+ is four. Taken together, these findings provide further evidence that gas-phase ion clustering studies find direct application in interpreting the structure of ions solvated in liquids.

Figure 6 also shows that a discontinuity in slope exists between the second and third Li^+ cluster. This feature may be due to steric hindrance. Although the very small lithium ion can easily attach one or two NH_3 groups, a further addition of ligands may lead to significant crowding about the central ion. Such an effect might necessitate rearrangement and an increase in average ligand-ion distances to accommodate other ligands in the first coordination shell. Further evidence that the ion clusters have a definite structure is revealed by comparing the entropy values given in Table III with ones expected[4] for a charged liquid drop. The magnitudes of the entropy data are considerably more negative than those for a disordered liquid drop, clearly indicating a rather more ordered structure for ammonia clustered about the alkali metal ions.

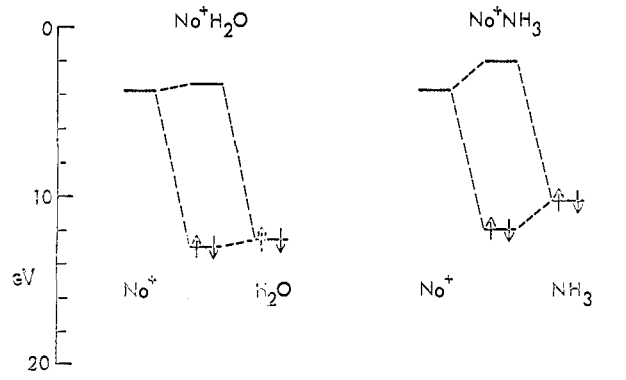

Figure 7. Qualitative molecular orbital scheme for Na^+H_2O and Na^+NH_3, showing interaction of lowest unfilled sodium and highest filled ligand orbitals. The highest unfilled Na^+ orbital is represented by the ionization potential of neutral sodium, whereas the positions of the ligand orbitals correspond to the ionization potentials of NH_3 and H_2O.

Electrostatic models have been quite useful in accounting for the relative binding energies of closed-shell systems, such as the alkali metal ions with water.[12] The bonding of open electronic shell ions is far stronger than for closed-shell ions of similar size,[6,7,9,10] indicating a high degree of covalent character. Differences between the bonding of various ligands to ions, and of ions in their relative ability to bond, are most apparent at the smallest cluster sizes and attention is focused on the binding properties of ions with a single ligand.

Although the ammonia and water molecules are isoelectronic and according to both transport and equation of state considerations[28] the effective sizes of these molecules are very similar, their dipole moments[15,16] and polarizabilities[29] are considerably different. The electrostatic interaction of closed-shell ions with these ligands may be represented by the potential:

$$\Phi = -\frac{e\mu}{r^2} - \frac{e^2\alpha}{2r^4} \tag{7}$$

where μ and α are, respectively, the dipole moment and polarizability of the ligand, e is the ionic charge, and r is the ion-ligand distance. Using internuclear distances of 1.84 Å for Li^+-O and 1.90 Å for Li^+-N from the ab initio calculations of Woodin et al.[14] water is calculated to be approximately 2–3 kcal/mol more strongly bound than ammonia. However, if the same internuclear distance (1.90 Å) is used in both cases, the opposite result is obtained. In order to establish the interatomic distances in a self-consistent fashion, a repulsive interaction of the form Ae^{-Br} is generally included.[12,24,30] However, parameters A and B are different for ammonia and water, and generally must be derived from separate empirical fits for each system under consideration. This reduces the usefulness of electrostatic calculations in predicting ligand bond energies.

The sensitivity of the results to the internuclear distance illustrates the inherent difficulty of this approach in predicting the relative bonding energy of various ligands. A simple molecular orbital model provides an attractive alternative for deducing the relative bonding strengths of various isoelectronic ligands to a particular ion. A qualitative molecular orbital approach has been used to predict the bonding properties of weakly bound neutral complexes[31,32] and molecular electron affinities.[33] The features of the model are illustrated in Figure 7 for the case of NH_3 and H_2O bound to Na^+. The highest unfilled Na^+ orbital is represented by the ionization potential

Table IV. Experimental Binding Energies of Ligands to K^+ and Relative Stabilities (Inverse Order of Ionization Potential Differences) Predicted by the Molecular Orbital Model

Ligand	$-\Delta H°$, kcal/mol[a]	ionization potential differences, eV[b]
NH_3	17.9	5.8
$MeNH_2$	19.1	5.1
Me_2NH	19.5	4.9
Me_3N	20.0	3.5
H_2O	16.9	8.3
Me_2O	20.8	5.7
Et_2O	22.3	5.2

[a] Experimental enthalpies from Davidson and Kebarle, ref 30. [b] Ionization potential of ligand, minus ionization potential of potassium, IP = 4.34; data taken from ref 34.

of neutral sodium, 5.14 eV,[34] whereas the positions of the ligand orbitals correspond to the ionization potentials of NH_3 and H_2O, 10.2 and 12.6 eV, respectively.[34] Since the 2p electrons of sodium have a binding energy of approximately 38 eV,[35] they should not interact appreciably with the ligand valence orbitals. The absolute energies of the cluster molecular orbitals cannot be inferred from the model and their positions in Figure 7 are only qualitative. However, the ion–ligand interaction is expected to be greater for NH_3 than H_2O, since there is a closer correspondence in energy between the highest filled orbital of the former ligand and the (empty) Na^+ level. This is in accord with the measured enthalpy data.

The rather wide applicability of this simple model is seen from Table IV, where a comparison is made of the experimental bond energies for a series of amines and ethers bound to K^+ with the relative order of stability predicted by the molecular orbital model. As with NH_3 vs. H_2O, the measured enthalpies fall in inverse order to the ion–ligand ionization potential differences. Although only qualitative trends can be predicted, the model avoids the necessity of making ab initio calculations for predicting relative bonding trends. This approach is able to predict the ordering of ion–ligand bond energies for many chemically similar systems, but may fail in a few cases, for example, the bonding order of Li^+ to methylamines where $NH_3 < MeNH_2 < Me_2NH$, Me_3N but $Me_3N < Me_2NH$.[24] However, the anomalous position of Me_3N in this series most likely arises from repulsive interactions between Li^+ and the methyl groups of the ligand,[24] a factor not accounted for in our simple model.

Deducing quantitative bond energies, as well as predicting the trends in the binding energies of dissimilar ligands to several types of ions, requires recourse to theoretical calculations. Although ab initio calculations offer the best method for ascertaining absolute values, other less expensive and less time-consuming methods can provide useful results. In this regard, we have employed the extended Hückel method[36] (semiempirical all valence molecular orbital calculations) to examine the relative differences in bonding of NH_3 and H_2O to the series of alkali metal ions Li^+, Na^+, K^+, and Rb^+. Although the extended Hückel method overestimates bonding energies, it often gives good results[36] when the energies are scaled to a system whose energy is well established.

In our calculations the coordinates of the H_2O and NH_3 ligands were taken from previous ab initio calculations[14] and then the ion–ligand distance was varied to minimize the energy. The off-diagonal elements of the effective Hamiltonian were calculated using the Wolfsberg–Helmholz arithmetic mean formula with $K = 1.75$. A consistent set of spectroscopic ionization potentials was used throughout.[37] Since the absolute binding energies obtained by the extended Hückel method are not in general reliable, all results were uniformly rescaled to agree with the experimental values for Na^+.

Table V. Binding Energies of Alkali Metal Ions, a Comparison of Extended Hückel Calculations with Experimental Enthalpies[e]

M^+	$\Delta(NH_3-H_2O)$, kcal/mol theory[a]	expt
Li^+	4.9	4.8[b]
Na^+	(5.1)	5.1[c]
K^+	2.5	2.2[d]
Rb^+	3.2	2.8[d]

[a] Extended Hückel calculations. All energies rescaled to Na^+. [b] From ref 22 and 23. [c] This work, see Table II, and ref 22. [d] From ref 10 and 22. [e] $\Delta(NH_3-H_2O)$ values are energy differences for M^+ bonding to NH_3 and H_2O.

Calculated bond energies are compared with experimental values for the alkali metal ions in Table V; the agreement is seen to be reasonably good. In each case the absolute binding energies show ammonia to be more the strongly bound ligand. In agreement with previous ab initio calculations[14] for Li^+NH_3 and Li^+H_2O, the M^+–N internuclear distance is found to be greater than the M^+–O distance. Our calculations also reveal little tendency for NH_3 and H_2O to donate charge to the metal ion. There is, however, slightly more charge transfer with NH_3 as ligand, a fact which accounts for the relative stability of the two ligands in their bonding to the alkali metal ions.

Conclusions

The relative bond strength of NH_3 to the various alkali metal ions is seen to vary inversely with their size, as expected. Only Li^+, the smallest of the series, displays evidence for a crowding effect around the center beyond the second ligand attachment, but both Li^+ and Na^+ display a tendency for a preferred first solvation shell coordination number of four.

The nature of the central ion is less important in the case of the large ions and no tendency for a solvation shell is noted from the bond energy data. For all ions, the successive attachment of ligands is expected to become progressively less dependent on the nature of the central ion, and eventually the energy of further ligand addition must asymptotically approach the heat of condensaton onto a microcroplet having a central positive charge. This tendency is seen from the data and is discussed elsewhere.[4]

Data for the relative bond strength of closed-shell ions with chemically similar ligands have been found to correlate with the difference in ionization potential between the ion and ligand. The general applicability of this model, particularly for ions of open electronic configuration, warrants further attention.

Acknowledgments. This research was sponsored by the Atmospheric Sciences Section of the U.S. National Science Foundation under Grant ATM 76-14914. The authors thank Drs. David Lewis and Naisin Lee for helpful discussions during the course of the work, and Mr. I. Tang and Mr. J. Davis for assistance in obtaining some of the data involving sodium ions. We are particularly indebted to Mr. Stephen Hogan for his invaluable technical assistance.

References and Notes

(1) See, for instance, P. Kebarle, S. K. Searles, A. Zolla, J. Scarborough, and M. Arshadi, *J. Am. Chem. Soc.*, **89**, 6393 (1967); W. R. Davidson and P. Kebarle, *ibid.*, **98**, 6125 (1976); P. Kebarle, *Annu. Rev. Phys. Chem.*, **28**, 445 (1977).
(2) B. S. Freiser and J. L. Beauchamp, *J. Am. Chem. Soc.*, **99**, 3214 (1977).
(3) A. W. Castleman, Jr., and I. N. Tang, *J. Chem. Phys.*, **57**, 3629 (1972).
(4) A. W. Castleman, Jr., P. M. Holland, and R. G. Keesee, *J. Chem. Phys.*, **68**, 1760 (1978).
(5) C. Tanford, *Proc. Natl. Acad. Sci. U.S.A.*, **71**, 1811 (1974); R. H. Ottewill, *J. Colloid Interface Sci.*, **58**, 357 (1977).
(6) I. N. Tang and A. W. Castleman, Jr., *J. Chem. Phys.*, **57**, 3638 (1972).
(7) I. N. Tang and A. W. Castleman, Jr., *J. Chem. Phys.*, **60**, 3981 (1974).

(8) I. N. Tang and A. W. Castleman, Jr., *J. Chem. Phys.*, **62**, 4576 (1975).
(9) I. N. Tang, M. S. Lian and A. W. Castleman, Jr., *J. Chem. Phys.*, **65**, 4022 (1976).
(10) A. W. Castleman, Jr., *Chem. Phys. Lett.*, **53**, 560 (1978).
(11) P. Kebarle in "Ion-Molecule Reactions", Vol. 1, J. L. Franklin, Ed., Plenum Press, New York, N.Y., 1972, Chapter 7.
(12) K. G. Spears, *J. Chem. Phys.*, **57**, 1850 (1972).
(13) See H. Kistenmacher, H. Popkie, and E. Clementi, *J. Chem. Phys.*, **54**, 5842 (1973); E. Clementi, "Lecture Notes in Chemistry", Vol. 2, "Determination of Liquid Water Structure, Coordination Numbers of Ions and Solvation for Biological Molecules", Springer-Verlag, New York, N.Y., 1976.
(14) R. L. Woodin, F. A. Houle, and W. A. Goddard III, *Chem. Phys.*, **14**, 461 (1976).
(15) D. K. Coles, W. E. Good, J. K. Bragg, and A. H. Sharbough, *Phys. Rev.*, **82**, 877 (1951).
(16) R. A. Robinson and R. H. Stokes, "Electrolyte Solutions", Butterworth, London, 1959, p 1.
(17) An arrangement often referred to as a "Kunsman source" [H. A. Barton, G. P. Harnwell, and K. H. Kunsman, *Phys. Rev.*, **27**, 739 (1926)] is produced by fusing a suitable coating onto a platinum filament. The coating used was a 1:2:1 mixture of respectively Al_2O_3 (J. T. Baker, "ultrex", U.H.P.), powdered quartz (J. T. Baker, reagent grade SiO_2), and the nitrate of the metal ion to be investigated (J. T. Baker, reagent grade). Filaments prepared in this manner gave copious ion currents (typically of the order of 1 mA) with little or no interference from other alkali species. The essential requirement for selective ion emission is high-purity coating materials; remaining impurities are readily exhausted by heating the freshly prepared filament for 1–5 h in vacuo. See also J. P. Blewett and E. J. Jones, *Phys. Rev.*, **50**, 464 (1936).
(18) P. Kebarle in "Interactions between Ions and Molecules", Vol. 6, P. Ausloos, Ed., Plenum Press, New York, N.Y., 1976, pp 459–487.
(19) A direct proportionality between intensity and activity may not be valid if the transmission of the quadrupole mass filter and ion optics varies with mass. Mass discrimination effects arise from transmitted ions which are injected off axis from the quadrupole filter or which have a nonzero transverse velocity component. The maximum acceptance area for off-axis ions varies as the inverse of the instrument resolution, whereas the maximum transverse energy for transmission is proportional to the full width at half maximum (fwhm) of the mass peak. In the Extranuclear Laboratories Model 162-8 spectrometer employed in these studies, it is possible to vary both resolution and fwhm in order to find a region of zero or very little mass discrimination.
(20) E. W. McDaniel and E. A. Mason, "The Mobility and Diffusion of Ions in Gases", Wiley, New York, N.Y., 1973.
(21) Since the ammonia and nitrogen concentrations are independent of time, and are much larger than those of the ion, integrating the forward reaction step gives $\ln [Li^+]/[Li^+]_0 = -k_f[NH_3][N_2]t$ where k_f is the termolecular rate constant for formation of Li^+NH_3 and $[Li^+]$, $[Li^+]_0$ are lithium ion concentrations at times t and $t = 0$, respectively. Typically, $k_f \sim 10^{-29}$ cm^6 molecule^2 s^{-1}; see, for example, K. G. Spears and E. E. Ferguson, *J. Chem. Phys.*, **59**, 4174 (1973). The transit time through the reaction cell is $t \sim 10^{-3}$ s; typically, for eq 5, $[NH_3] \sim 10^{-2}$ $[N_2] \sim 10^{15}$ molecule/cm^{-3}. At the sampling orifice, therefore, $[Li^+] \sim 0.4[Li^+]_0$, which indicates insufficient encounters of Li^+ with NH_3 to allow a true equilibrium situation to develop. Measurements on clusters other than the first were made at significantly higher ammonia concentrations and lower temperatures. Since most ion–molecule reactions exhibit a negative temperature dependence, both of these conditions facilitate the formation of Li^+NH_3. Consequently, eq 5 is not a rate-determining process in our experimental studies of larger cluster species.
(22) I. Dzidić and P. Kebarle, *J. Phys. Chem.*, **74**, 1466 (1970).
(23) R. H. Staley and J. L. Beauchamp, *J. Am. Chem. Soc.*, **97**, 5920 (1975).
(24) R. L. Woodin and J. L. Beauchamp, *J. Am. Chem. Soc.*, **100**, 501 (1978).
(25) A. Hinchcliffe and J. C. Dobson, *Theor. Chim. Acta*, **39**, 17 (1975).
(26) J. D. Payzant, A. J. Cunningham, and P. Kebarle, *Can. J. Chem.*, **51**, 3242 (1973).
(27) P. Gans and J. B. Gill, *J. Chem. Soc., Dalton Trans.*, 779 (1976).
(28) J. O. Hirschfelder, C. F. Curtiss, and R. B. Bird, "Molecular Theory of Gases and Liquids", Wiley, New York, N.Y., 1954.
(29) R. C. Weast, Ed., "Handbook of Chemistry and Physics", 57th ed, Chemical Rubber Publishing Co., Cleveland, Ohio, 1976.
(30) W. R. Davidson and P. Kebarle, *J. Am. Chem. Soc.*, **98**, 6133 (1976).
(31) S. E. Novick, S. J. Harris, K. C. Janda, and W. Klemperer, *Can. J. Phys.*, **53**, 2007 (1975).
(32) M. Trenary, H. F. Schaefer III, and P. Kollman, *J. Am. Chem. Soc.*, **99**, 3885 (1977).
(33) J. P. Lowe, *J. Am. Chem. Soc.*, **99**, 5557 (1977).
(34) V. I. Vedeneyev, L. V. Gurvich, V. N. Kondrat'yev, V. A. Medvedev, and Ye. L. Frankevich, "Bond Energies, Ionization Potentials and Electron Affinities", Arnold, London, 1966.
(35) J. C. Slater, *Phys. Rev.*, **98**, 1039 (1955).
(36) G. H. Wagnière, "Introduction to Elementary Molecular Orbital Theory and Semiempirical Methods", Lecture Notes in Chemistry, Vol. 1, Springer-Verlag, New York, N.Y., 1976.
(37) O. P. Tcharkin, G. B. Bobykina, and M. E. Dyatkina in "Molecular Structure and Quantum Chemistry", Naukova Dumka, Kiev, 1970, p 155; O. P. Tcharkin and M. E. Dyatkina, *ibid.*, p 163.

Direct Mixture Analysis by Mass-Analyzed Ion Kinetic Energy Spectrometry Using Negative Chemical Ionization

Gary A. McClusky, Richard W. Kondrat, and Robert G. Cooks*

Contribution from the Department of Chemistry, Purdue University, West Lafayette, Indiana 47907. *Received February 27, 1978*

Abstract: Negative ions, generated by chemical ionization and isolated by mass analysis, can be dissociated by collision to yield either positively or negatively charged fragments both of which are characteristic of particular functional groups. These MIKE spectra have comparable S/N characteristics to those of selected positively charged ions and they form the basis for the characterization of specific components in complex mixtures (such as glucose in urine) without any sample pretreatment. Isomeric compounds can frequently be distinguished and it is shown that the charge stripping reaction ($m_1^- \rightarrow m_1^+$) can be more sensitive to different isomers than is collision-induced dissociation. Sensitivity is better than 10^{-10} g with the highest sensitivity being obtained in the single reaction monitoring mode in which a selected reaction of a chosen ion is monitored as a function of time. The detection limit is lower in the MIKES method than in conventional mass spectrometry and this is accounted for by the decreased chemical noise in MIKES.

A recently developed alternative to combined chromatography/mass spectrometry for the analysis of mixtures is direct analysis in a two-stage mass spectrometer.[1] The first stage functions as an ion separator and the second as an ion identifier. The best developed[2-5] of the various instrumental permutations which fall within this protocol is that in which ionization is by chemical ionization (CI), separation is by a sector magnetic field, fragmentation is by collision-induced dissociation (CID), and fragment ion analysis is by a sector electrostatic analyzer. This specific set of choices[6] represents the use of a reversed-sector MIKE spectrometer (mass-analyzed ion kinetic energy spectrometer). Hallmarks of this analytical procedure are that little or no workup of complex samples is required, while good sensitivity with specificity of compound identification is obtained.

All previously reported work on the direct two-stage analysis of mixtures has employed positive ions.[1-3] Our objectives here include an investigation of the potential of negative ions in such analyses. In addition, we have sought to introduce more selectivity and specificity into the direct analysis protocol at two points: (1) the ionization process; (2) the types of ion/molecule reactions used to characterize the selected ion. It is well known

0002-7863/78/1500-6045$01.00/0